Charge Equilibration via Neural Network Techniques (CENT)

Somayeh Faraji

Institute for Advanced Studies in Basic Sciences (IASBS), Zanjan

2nd workshop on Machine Learning in Physics,
University of Tehran, Tehran
October 5, 2018

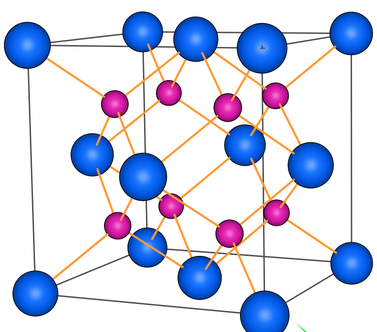

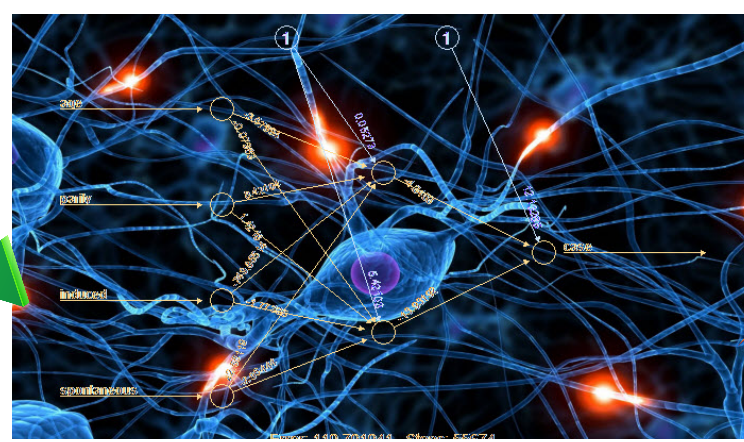

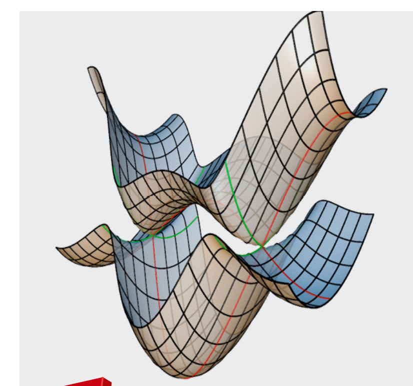

Charge transfer at organic/metal interfaces

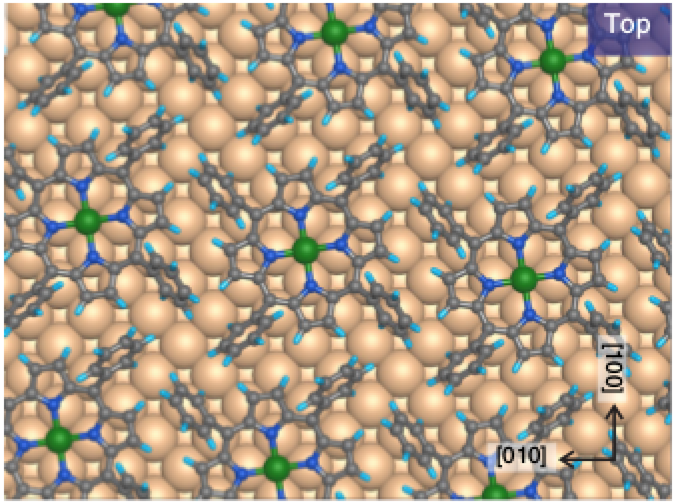

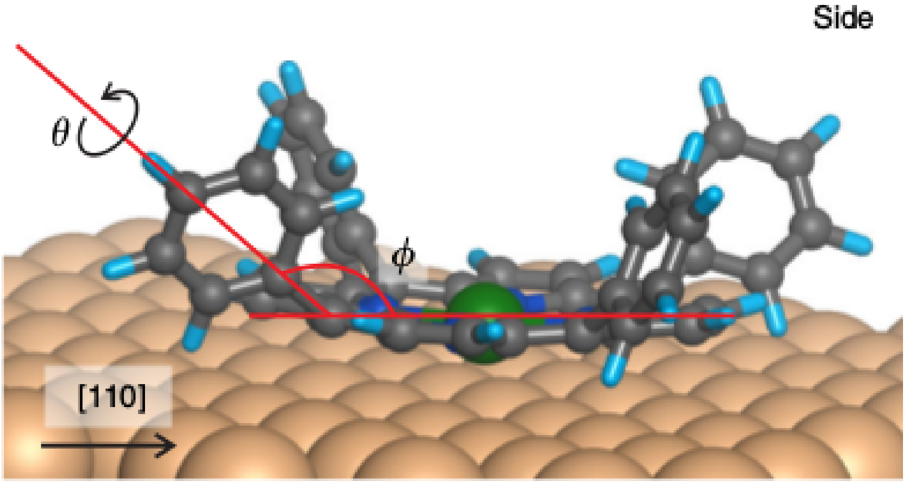

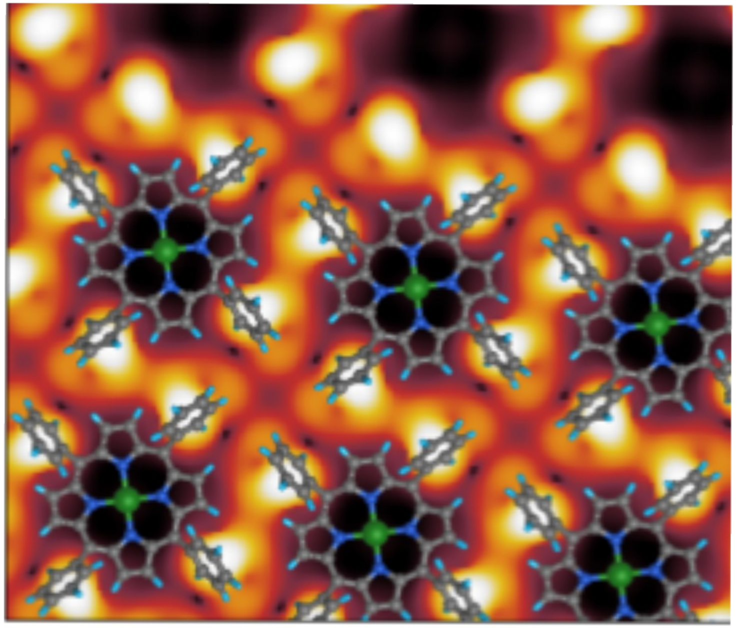

Multi-orbital charge transfer at nickel tetraphenyl porphyrin molecules adsorbed on Cu(100)

G. Zambolini *et. al.* Nature Communications, **8**, 335 (2017)

DFT and the Hellmann Feynman Theorem

$$\hat{H}_{tot}\psi(\mathbf{r},\mathbf{R}) = E\psi(\mathbf{r},\mathbf{R})$$

Born-Openheimer approximation:

$$\left(\hat{H}_e(\{\mathbf{R}\}) - E_e(\{\mathbf{R}\})\right)\psi_e(\mathbf{r};\mathbf{R}) = 0 \;\; where \;\; \hat{H}_e = \hat{T}_e + \hat{V}_{ee} + \hat{V}_{e-I}$$

Hohenberg-Kohn theorems:

$$E[\rho] = T[\rho] + \int \rho(\mathbf{r})V_{ext}(\mathbf{r})d\mathbf{r} + E_{int}[\rho]$$

Kohn-Sham equations:

$$E_{KS} = -\sum_{i=1}^{occ}\frac{|\nabla_i^2|}{2} + \int V_{ext}(\mathbf{r})\rho(\mathbf{r})d\mathbf{r} + \frac{1}{2}\int\int\frac{\rho(\mathbf{r})\rho(\mathbf{r}\prime)}{|\mathbf{r}-\mathbf{r}\prime|}d\mathbf{r}d\mathbf{r}\prime + E_{xc}[\rho(\mathbf{r})]$$

$$[-\frac{1}{2}\nabla^2 + V_{ext}(\mathbf{r}) + V_H(\mathbf{r}) + V_{xc}(\mathbf{r})]\psi_i(\mathbf{r}) = \varepsilon_i\psi_i(\mathbf{r})$$

$$E_{gs}(\{\mathbf{R}\}) = \sum_{i=1}^{occ}\varepsilon_i - \int\rho(\mathbf{r})V_{xc}(\mathbf{r})d\mathbf{r} + \frac{1}{2}\int\int\frac{\rho(\mathbf{r})\rho(\mathbf{r}\prime)}{|\mathbf{r}-\mathbf{r}\prime|}d\mathbf{r}d\mathbf{r}\prime + E_{xc}[\rho]$$

Hellmann Feynmann theorem

$$F = -\int\frac{\rho(\mathbf{r}')(\mathbf{r}-\mathbf{r}')}{|\mathbf{r}-\mathbf{r}'|^3}d\mathbf{r}'$$

A neural network scheme for ionic systems based on charge equilibration method

Introduction

Methods

CENT

Applications

$$U_{tot}(\{q_i\}) = \sum_{i=1}^{N}\left(E_i^0 + \chi_i q_i + \frac{1}{2}J_{ii}q_i^2\right) + \frac{1}{2}\int \frac{\rho(\mathbf{r})\rho(\mathbf{r}')}{|\mathbf{r}-\mathbf{r}'|}\,d\mathbf{r}\,d\mathbf{r}'$$

Simplest atomic charge distribution: Gaussian

$$\rho_i(\mathbf{r}) = \frac{q_i}{\alpha_i^3\pi^{\frac{3}{2}}}\exp\left(-\frac{|\mathbf{r}-\mathbf{R}_i|^2}{\alpha_i^2}\right)$$

Resulting analytic energy expression:

$$U_{tot}(\{q_i\},\{\mathbf{R}_i\}) = \sum_{i=1}^{N}\left(E_i^0 + \chi_i q_i + \frac{1}{2}(J_{ii} + \frac{2\gamma_{ii}}{\sqrt{\pi}})q_i^2\right) + \sum_{i>j}^{N} q_i q_j \frac{erf(\gamma_{ij}R_{ij})}{R_{ij}}$$

$$\gamma_{ij} = \frac{1}{\sqrt{\alpha_i^2+\alpha_j^2}}$$

Ghasemi et al., Phys. Rev. B **92**, 045131 (2015)

Charge equilibration process

$$\frac{\partial U_{tot}}{\partial q_i} = 0, \forall i = 1, ..., N \Rightarrow \sum_{j=1}^{N} A_{ij} q_j + \chi_i = 0.$$

where

$$A_{ij} = \begin{cases} J_{ii} + \frac{2\gamma_{ii}}{\sqrt{(\pi)}} & \text{for } i = j \\ \frac{erf(\gamma_{ij} r_{ij})}{r_{ij}} & \text{for } i \neq j \end{cases}$$

Adding the constraint total charge via the Lagrange multipliers leads

$$q_{tot} = \sum_i^N q_i \qquad \tilde{A}\mathbf{Q} = -\chi$$

$$\left(\begin{array}{ccc|c} & & & 1 \\ & A_{i,j} & & \vdots \\ & & & 1 \\ \hline 1 & \dots & 1 & 0 \end{array} \right) \left(\begin{array}{c} q_1 \\ \vdots \\ q_N \\ \hline \lambda \end{array} \right) = \left(\begin{array}{c} -\chi_1 \\ \vdots \\ -\chi_N \\ \hline q_{tot} \end{array} \right)$$

Schematic illustration of the charge equilibration via neural network technique (CENT)

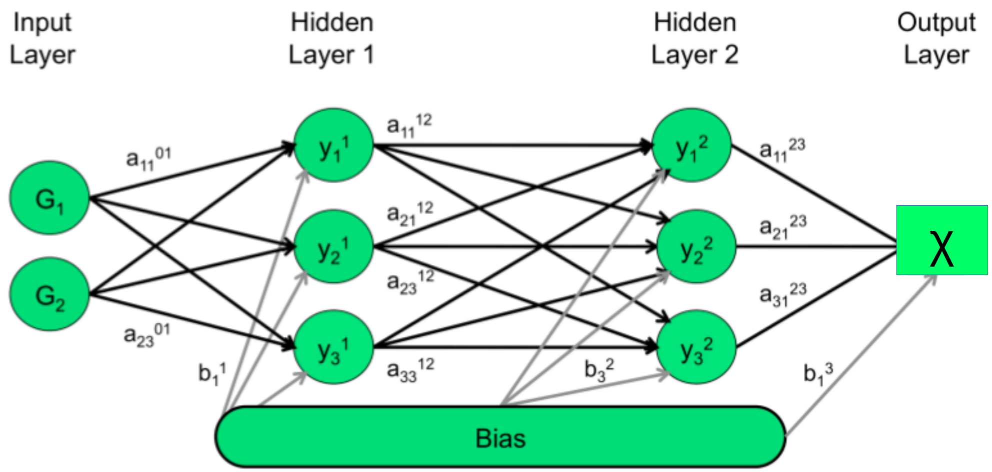

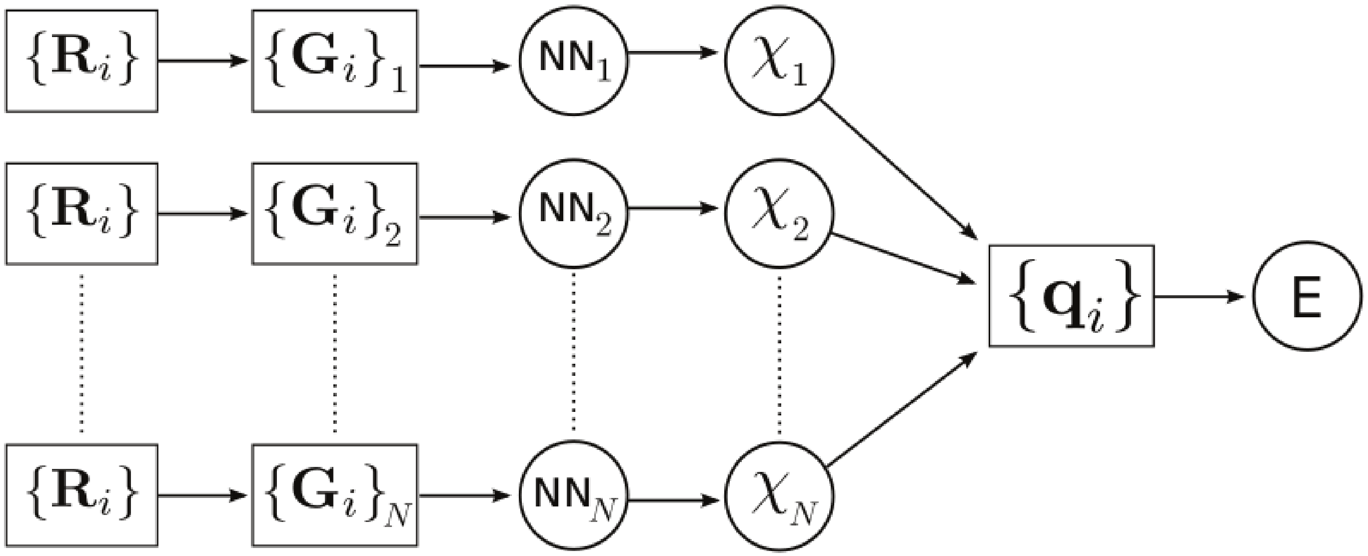

- Explicit short range environment dependence of the χ_i's.
- Implicit long range environment dependence of the q_i's.

Transferability: Testing CENT for bulk CaF_2

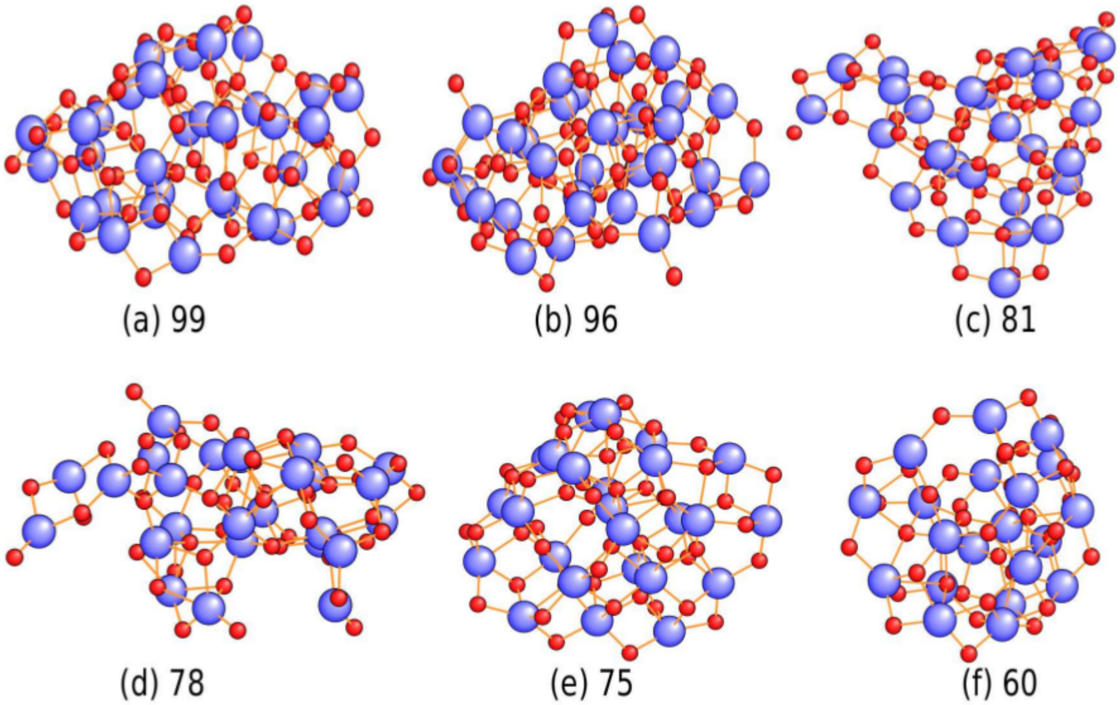

- 2800 data points during the training process
    - *FHI-aims* all-electron full-potential code
    - PBE xc-functional

Transferability: Testing CENT for bulk CaF_2

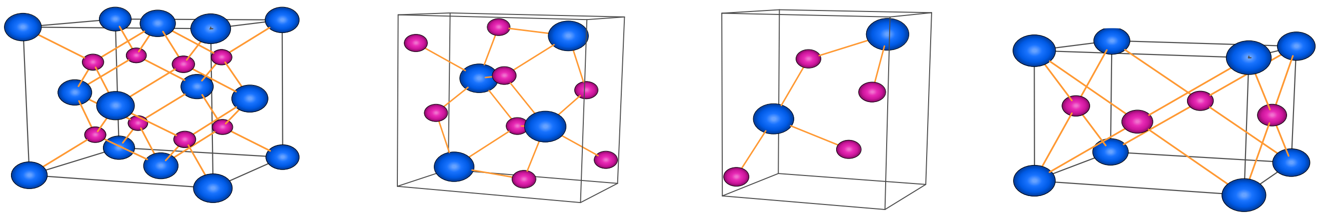

(a) Fm-3m (b) Pnma (c) Pmc21 (d) P4/mmm

- **Transferability**
  - Bulk properties (lattice constants, elastic properties etc.)
  - Heat capacities
  - Structural phase transition at high pressure
  - Phonon dispersion of fluorite structure
  - Vacancies in fluorite structure
  - Surfaces of fluorite structure

  - **DFT**
    - PBE (XC functional used for reference data points)
    - LDA
  - **Born-Mayer-Huggins (BMH) potential**

The average errors of formation energies

CENT: 1 % LDA: 11 % BMH: 56 %

Structural phase transition at high pressure

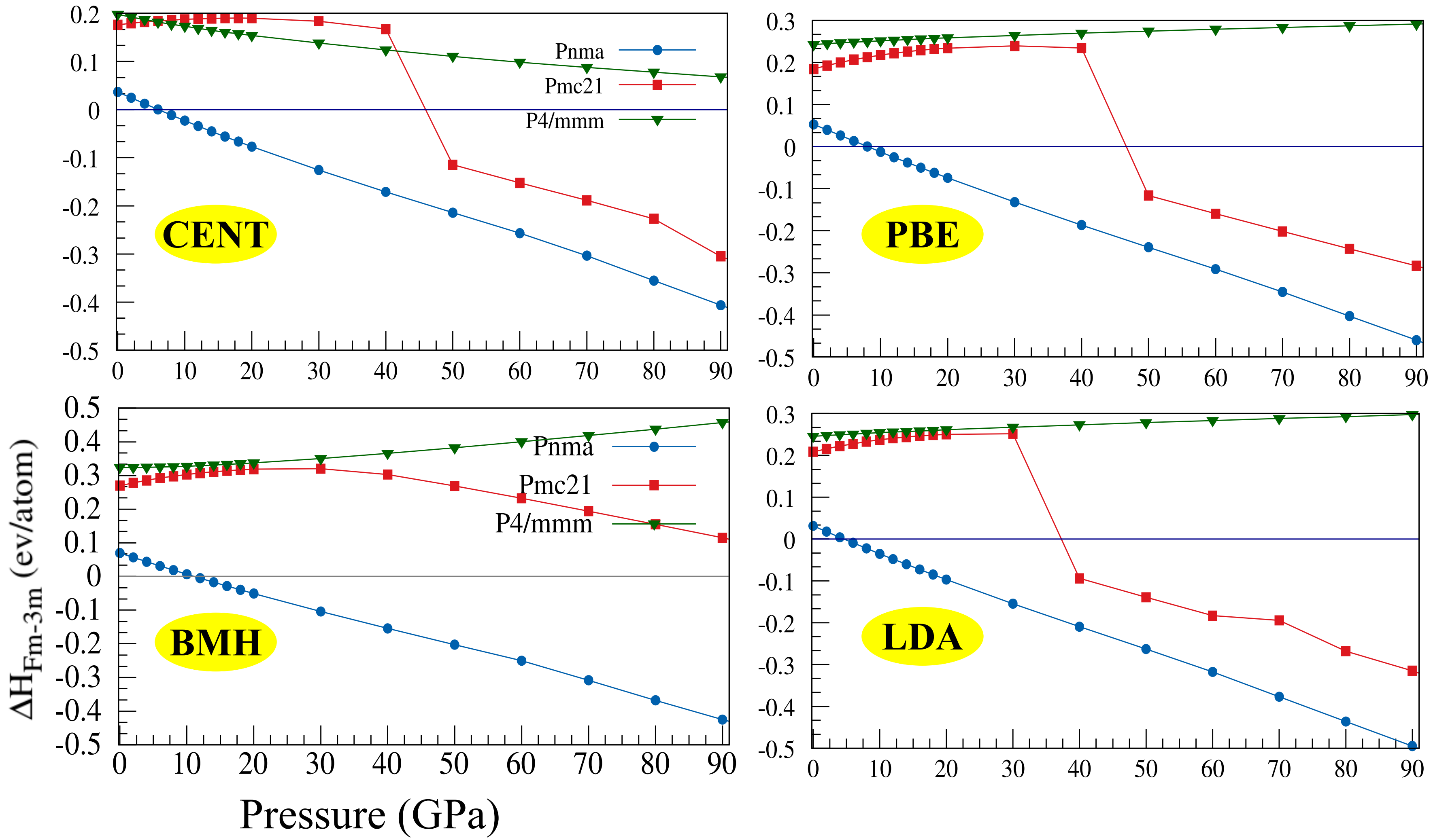

Phonon dispersion of fluorite structure

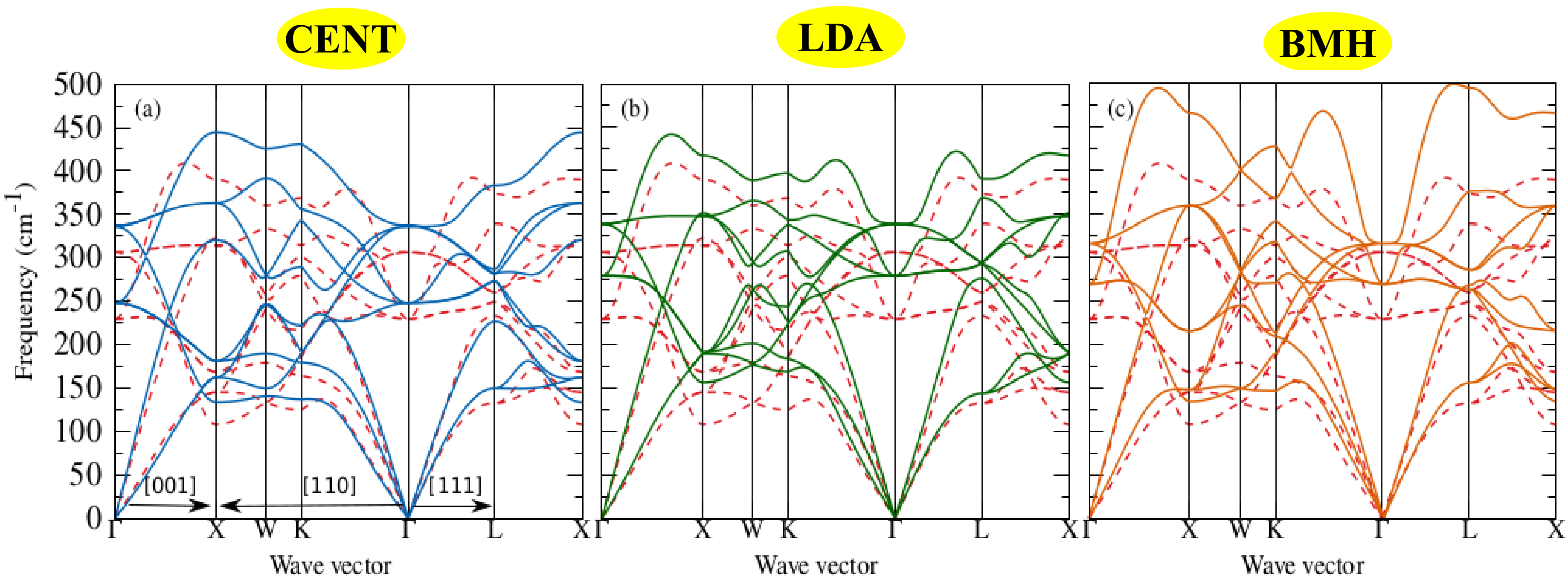

- Phonopy code is used for the calculation of phonon dispersion
- Acoustic modes: CENT results agrees with those of PBE
- Optical modes: results of all methods are the same qualitatively and
- differ from each other quantitatively

New Crystal Phase of CaF_2

- **New Found Crystal Phase**
  - **Space group: P-62m**
  - **Lattice vectors from PBE (in Ang):**
    a:(3.55, 0, 0)
    b:(0, 6.09,0)
    c:(0, 3.04, 5.28)

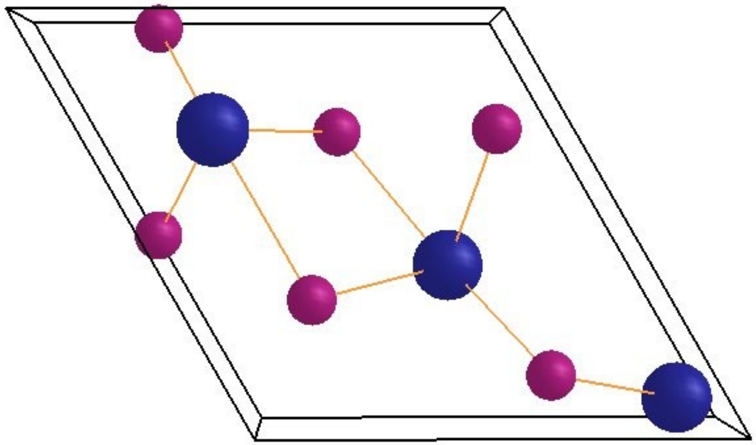

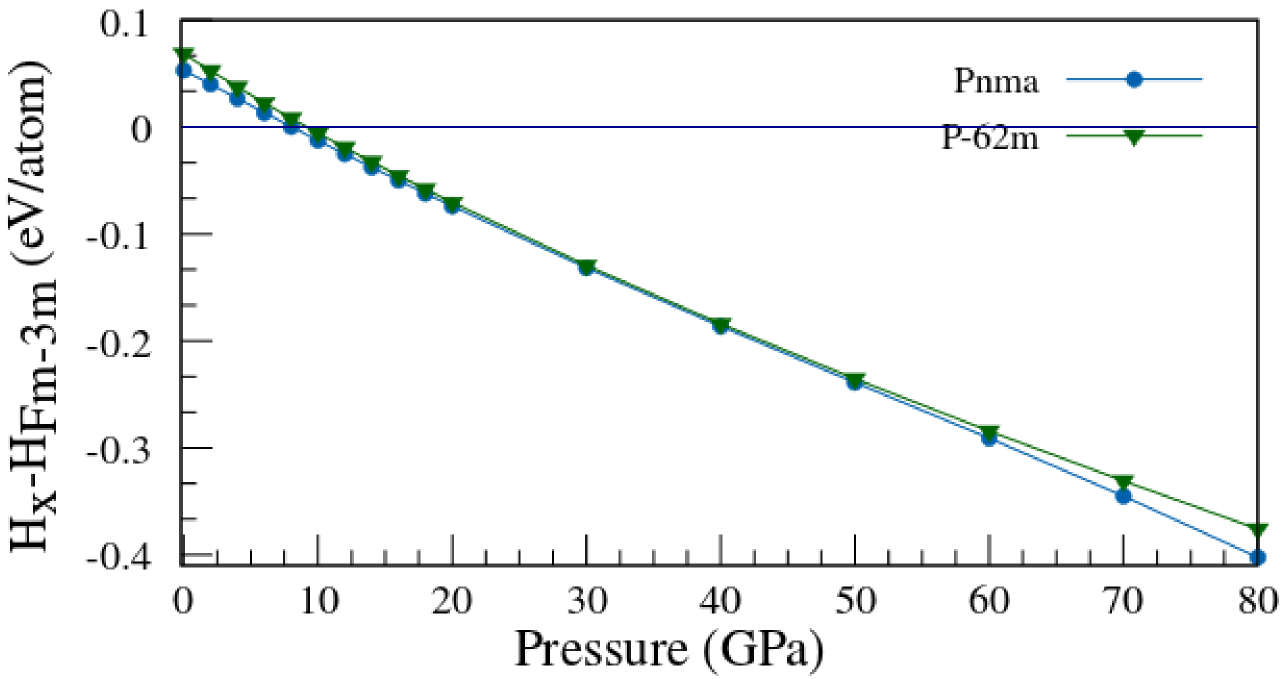

Energy landscape of ZnO

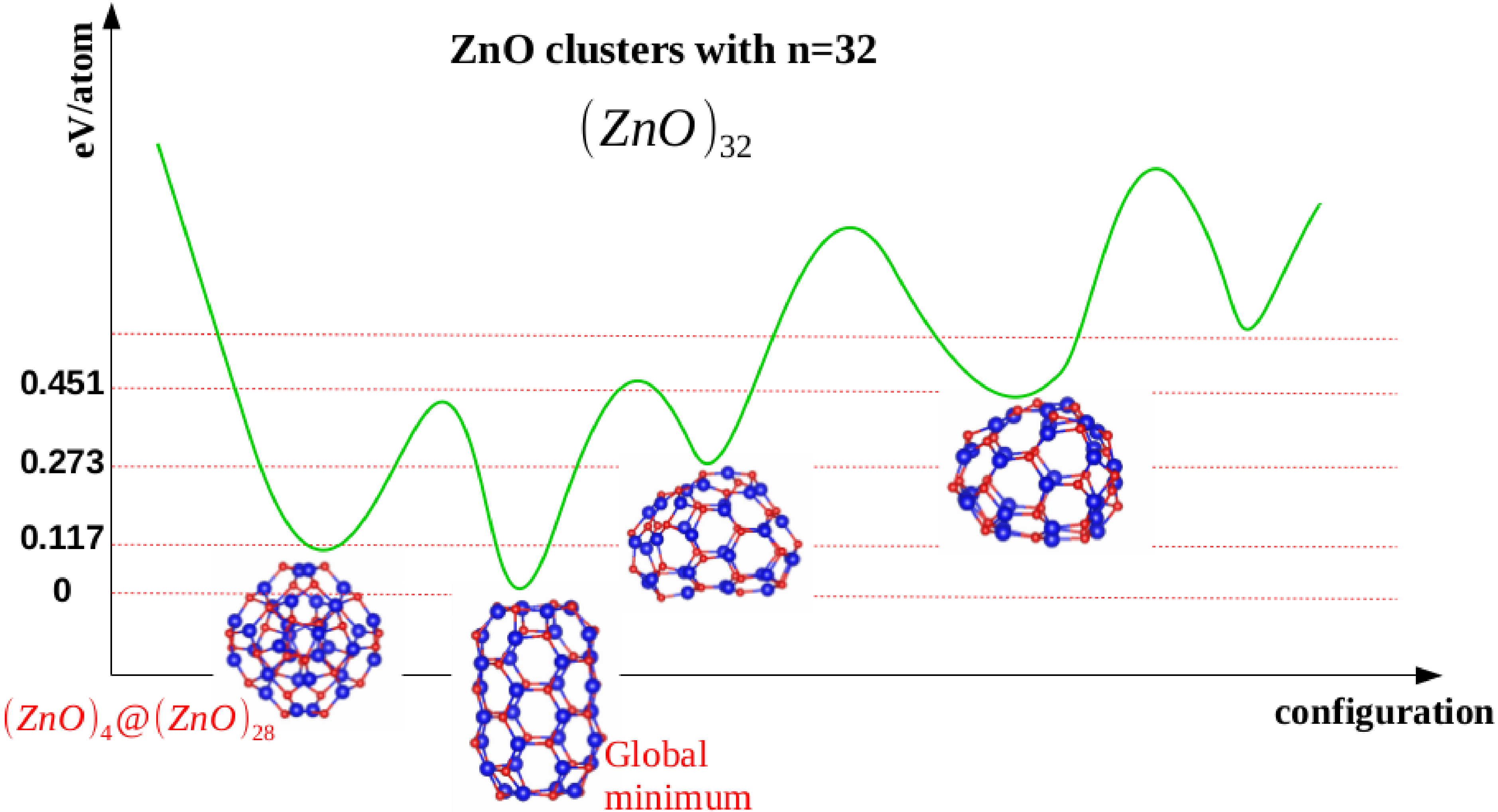

R. Rasoulkhani et. al, Rhys. Rev. B **96**, 064108 (2017).

Energy landscape of ZnO

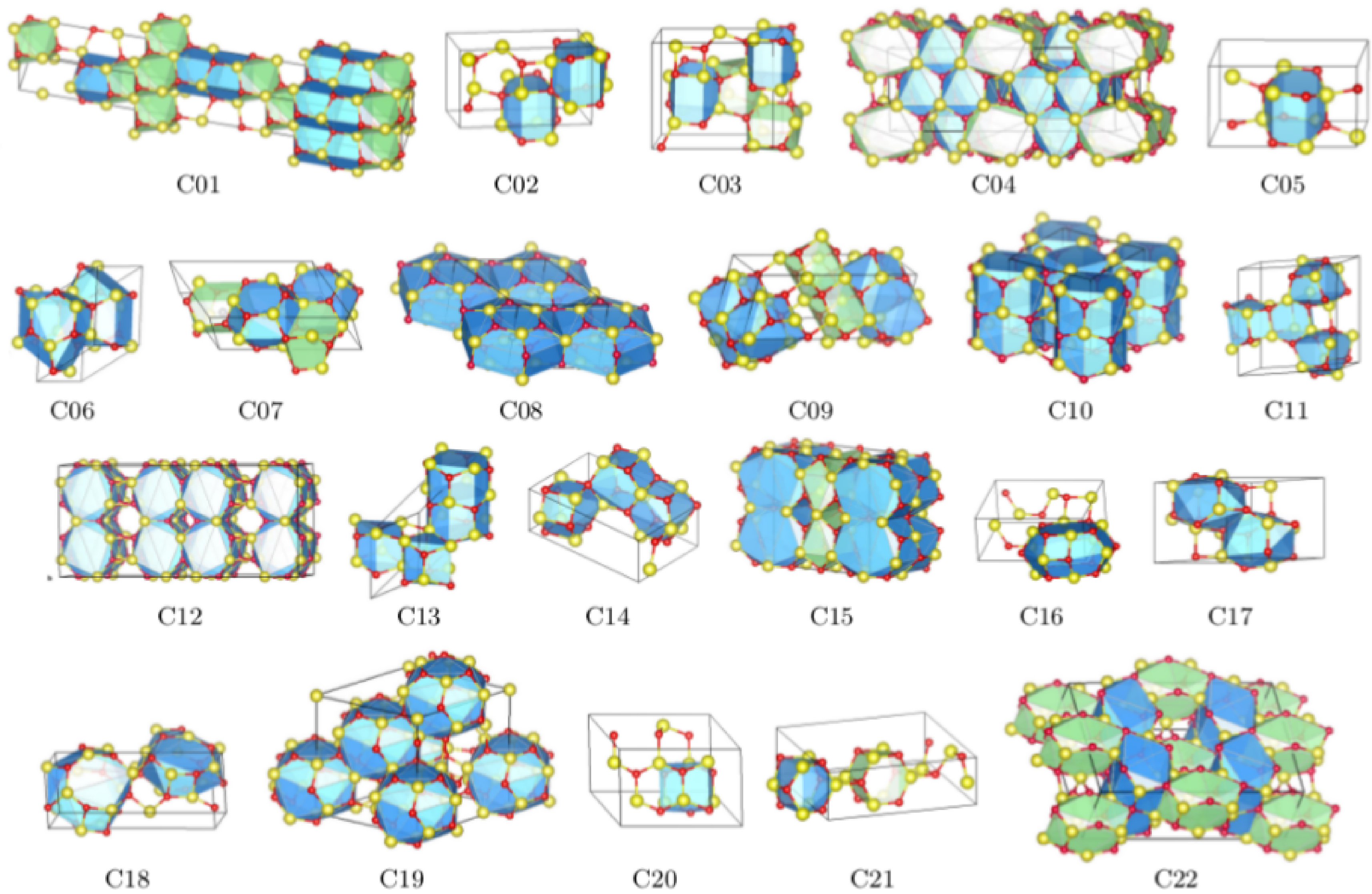

R. Rasoulkhani et. al, Rhys. Rev. B **96**, 064108 (2017).

Phonon dispersion of new phases of ZnO

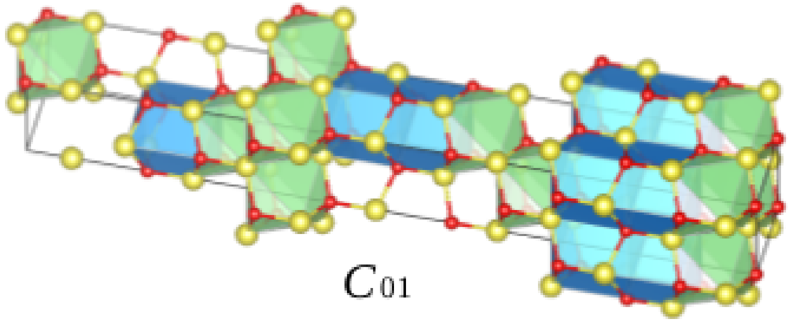

C_{01}

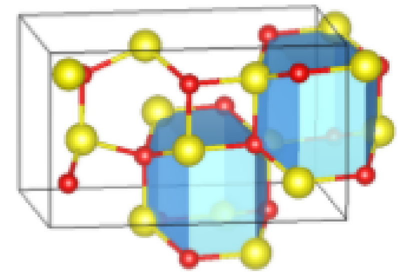

C_{02}

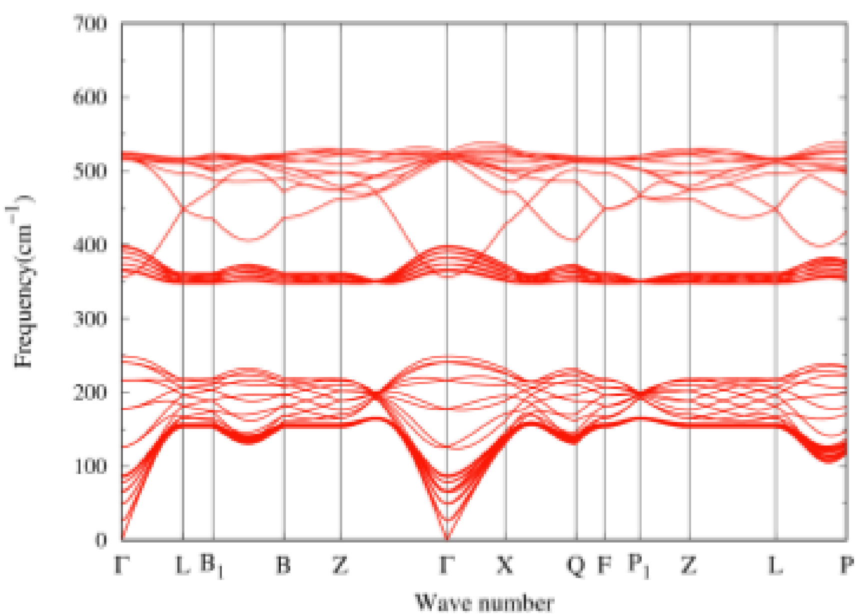

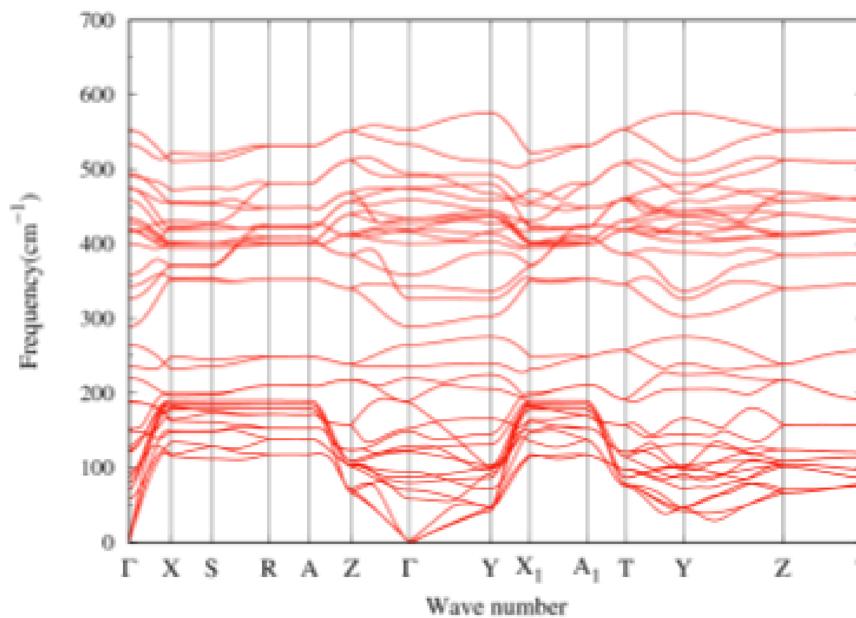

Two-dimensional hexagonal nano sheet(HNS) of TiO_2

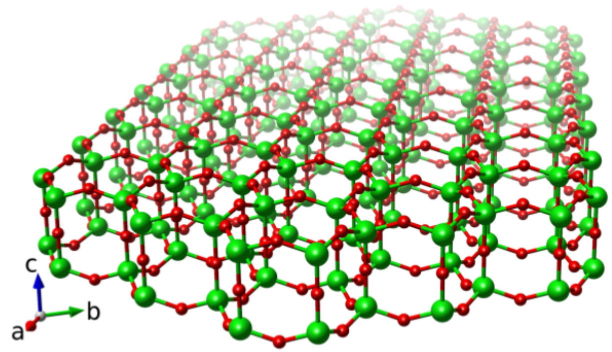

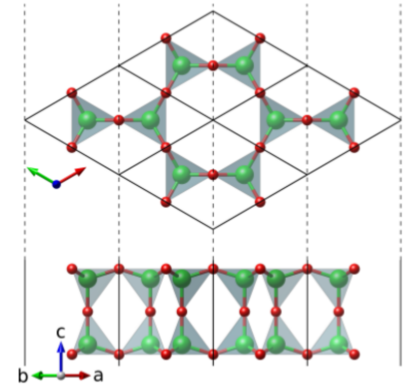

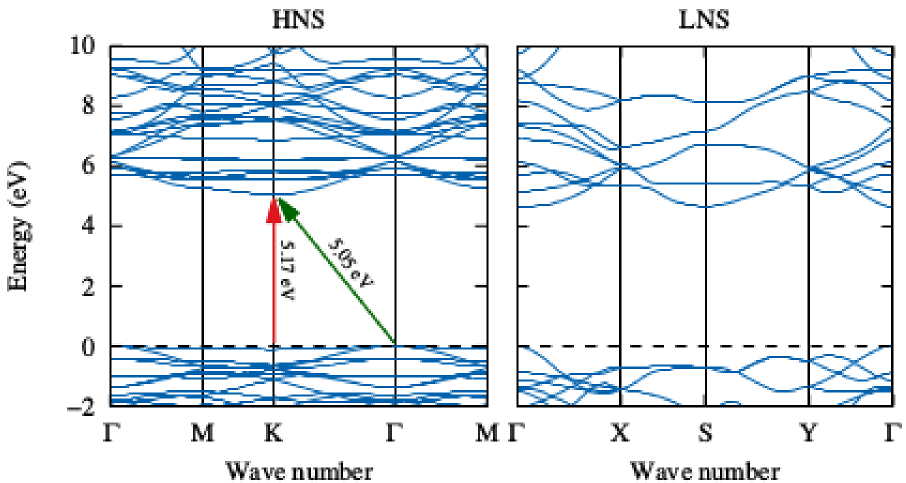

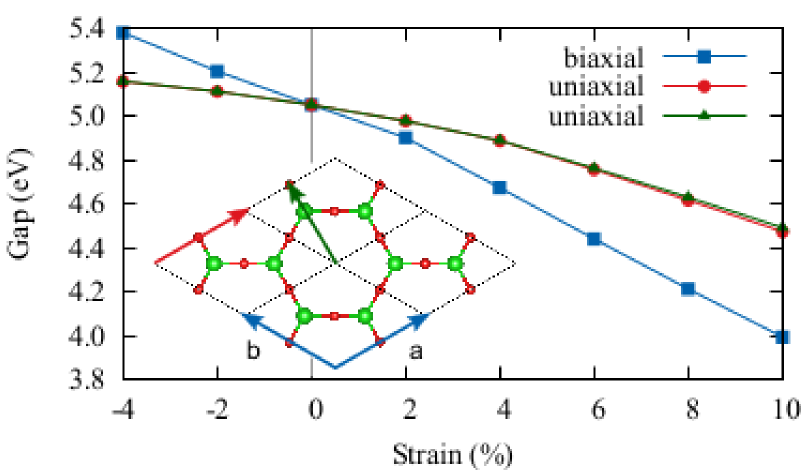

Thank you...